Army Research Laboratory
Aberdeen Proving Ground, MD 21005-5068

ARL-TR-0000 **November 2010**

Experimental Methodology using Digital Image Correlation (DIC) to Assess Ballistic Helmet Blunt Trauma

Dixie Hisley, James Gurganus, Joseph Lee*, Scott Williams, Andrew Drysdale
Survivability/Lethality Analysis Directorate, ARL,
***Bowhead Technical and Professional Services, Inc.**

Report Documentation Page

Form Approved
OMB No. 0704-0188

1. REPORT DATE	2. REPORT TYPE	3. DATES COVERED
NOV 2010		**00-00-2010 to 00-00-2010**

4. TITLE AND SUBTITLE	5a. CONTRACT NUMBER
Experimental Methodology Using Digital Image Correlation (DIC) To Assess Ballistic Helmet Blunt Trauma	5b. GRANT NUMBER
	5c. PROGRAM ELEMENT NUMBER
6. AUTHOR(S)	5d. PROJECT NUMBER
	5e. TASK NUMBER
	5f. WORK UNIT NUMBER
7. PERFORMING ORGANIZATION NAME(S) AND ADDRESS(ES) **Army Research Laboratory,Aberdeen Proving Ground,MD,21005**	8. PERFORMING ORGANIZATION REPORT NUMBER
9. SPONSORING/MONITORING AGENCY NAME(S) AND ADDRESS(ES)	10. SPONSOR/MONITOR'S ACRONYM(S)
	11. SPONSOR/MONITOR'S REPORT NUMBER(S)

12. DISTRIBUTION/AVAILABILITY STATEMENT
Approved for public release; distribution unlimited

13. SUPPLEMENTARY NOTES

14. ABSTRACT
As modern helmets have become quite capable of defeating the penetration capabilities of ballistic threats, Soldiers may experience head injuries due to blunt trauma caused by helmet back face deformation (BFD). Possible resulting injuries include skull fracture, hematoma, concussion,contusion, diffuse axonal injury, etc. Some of these injuries have been associated with traumatic brain injury.

15. SUBJECT TERMS

16. SECURITY CLASSIFICATION OF:			17. LIMITATION OF ABSTRACT	18. NUMBER OF PAGES	19a. NAME OF RESPONSIBLE PERSON
a. REPORT **unclassified**	b. ABSTRACT **unclassified**	c. THIS PAGE **unclassified**	**Same as Report (SAR)**	**30**	

Abstract

As modern helmets have become quite capable of defeating the penetration capabilities of ballistic threats, Soldiers may experience head injuries due to blunt trauma caused by helmet back face deformation (BFD). Possible resulting injuries include skull fracture, hematoma, concussion, contusion, diffuse axonal injury, etc. Some of these injuries have been associated with traumatic brain injury.

In order to assess potential injury mechanisms prior to fielding new helmets, we have developed a means to experimentally replicate and measure helmet BFD that can be correlated to injury criteria. In this study, helmet performance test methodology is developed using a digital image correlation (DIC) technique. DIC provides the capability to measure dynamic displacements, thereby, providing the ability to calculate deformation, velocity and acceleration rates. We have shown that digital image correlation is an experimentation technique that accurately captures BFD area and rate of deformation for impacts against combat helmets. We used the DIC data to calculate a new metric; the available energy that could potentially impact a Soldiers head, thus, showing that DIC can be used to provide dynamic helmet performance data that will allow increased understanding of BFD and quantitative assessment and validation of helmet performance results.

Our study shows that DIC data upholds the hypothesis that helmet BFD mechanically loads the skull similar to a direct impact from a less-than-lethal projectile or blunt object impact. The available energy obtained from DIC measurements was used to calculate the blunt criterion (BC) for helmet standoff distances of .5 in and .75 in, which in turn can provide a prediction of the probability of abbreviated injury scale (AIS) levels and, in particular, skull fracture.

Knowledge of the conditions leading to head trauma obtained through experimentation or numerical modeling should enable the selection of new energy-absorbing materials for helmets. The ultimate goal of future instrumentation and methodology efforts should allow helmet design candidate performances to be objectively evaluated. Test data and characterization of helmet response could then be used to achieve improved warfighter survivability.

Report Documentation Page

Insert the “Report Documentation Page” here.

Contents

List of Figures v

List of Tables vi

1. Introduction 1
1.1 Helmet Back Face Deformation (BFD) and Behind Armor Blunt Trauma (BABT) . . . 1
1.2 Experimentation Techniques for Replicating and Measuring Helmet BFD 2

2. Objectives 2

3. Approach/Methods 3
3.1 Criteria to Predict Blunt Impact Injury and Guide Experimentation 3
3.2 DIC Concepts 4
3.2.1 Calibration 4
3.2.2 Noise Floor 5
3.3 Gaining Experience with DIC using Pendulum Impacts 5
3.3.1 Pendulum Impacts on Cardboard 6
3.3.2 Pendulum Impacts on Copper 6
3.4 Range and DIC Set-up for 9 mm Impacts on Helmets 7
3.4.1 Helmet Mounting Technique 8
3.4.2 Surface Preparation, Dot Pattern, and Lighting 9

4. Results and Discussion 9
4.1 Overview of DIC Tests for 9 mm Shots Against Helmets 9
4.2 Available Energy for Potential Impact to Solider's Head 10
4.3 Using DIC Measurements to Calculate Energy for Blunt Criterion 11
4.4 BFD Velocity Surface Plot 13
4.5 Summary of Helmet Results 14
4.6 Similarity of Helmet BFD to Blunt Object Impact 16

5. Conclusions 16

6. Recommendations 17

7. References 18

List of Symbols, Abbreviatons, and Acronyms 21

Distribution List **23**

List of Figures

Figure 1. Dynamic (increasing time left to right) development of helmet back-face deformation 1
2 Hypothesis question: Is helmet BFD similar to blunt impact? 2
Figure 3. Noise floor measurement 5
Figure 4. DIC image for cardboard impact (a) before tearing (b) after tearing 6
Figure 5. DIC and FARO® images for copper plate impact 7
Figure 6. Range schematic for 9mm shots against helmets 8
Figure 7. Process of small arms penetration into a composite laminate 10
Figure 8. Dissected helmet and mushroomed 9mm bullet 11
Figure 9. DIC deformation contours for 9 mm impact (a) at helmet standoff (b) at maximum deformation 12
Figure 10. DIC time histories and surface contours for 9 mm impact (a) at helmet standoff (b) at maximum deformation 13
Figure 11. BFD velocity surface plot 13
Figure 12. Cumulative available energy, effective area and BC time histories 15
Figure 13. Helmet BFD similar to blunt object impact 16

List of Tables

Table 1. Summary of helmet tests 9
Table 2. Summary of helmet results 14

1. Introduction

As modern helmets and body armor have become quite capable of defeating the penetration capabilities of ballistic threats, Soldiers are surviving injuries that would have been potentially fatal in previous wars. However, Soldiers may now experience injuries due to behind armor blunt trauma (BABT) *(1–3)* . For example, a .44 Magnum has almost twice the energy of all the other calibers identified under Henry Packard White Test Procedure Level IIIA for helmets (*4*). The helmet will stop the projectile, but the resultant blunt trauma is likely to cause serious injury (*5*). When the impact energy of a threat on a helmet is converted to other forms of energy, one potential phenomenon that can occur is helmet back face deformation (BFD).

1.1 Helmet Back Face Deformation (BFD) and Behind Armor Blunt Trauma (BABT)

BFD is defined as the maximum displacement of personal armor during impact. During non-perforating bullet impacts, as shown in figure 1, a potential reaction mechanism of composite helmets is interior surface delamination and deformation. The red cross in figure 1 identifies the center of the BFD as it develops with increasing time. If the deformation exceeds the helmet

Figure 1. Dynamic (increasing time left to right) development of helmet back-face deformation.

standoff (distance from helmet to head), it can transfer large forces to the skull, potentially causing injury termed BABT. Even if the helmet completely stops the bullet with no BFD, other indirect injury mechanisms are possible to the head and neck due to forces from oblique impacts. These mechanisms are not well understood. Thus, correlation of injury from physical measurements is difficult, since there is no accepted consensus on head injury criteria for inclusion in DoD and law enforcement standards. In order to assess potential injury mechanisms prior to fielding new helmets, we need to develop a means to experimentally replicate and measure helmet BFD so that it can be correlated to injury criteria. This effort is particularly important as the U.S. Army's Soldiers face small arms threats with increasing lethality, and as we try to decrease the weight of the helmet.

A goal of this study is to develop experimentation methodology that can produce a wide range of robust, accurate, repeatable time-dependent helmet BFD data for use by the modeling and simulation, and medical communities as they develop a better understanding of injury mechanisms. Thus, we are developing an experimental procedure ahead of specific data requirements from these communities.

1.2 Experimentation Techniques for Replicating and Measuring Helmet BFD

A promising experimentation technique for helmet test methodology and the subject of this report is digital image correlation (DIC) – a non-contact, optical technique that can be used to measure three-dimensional (3-D) deformations. DIC can provide area or volume of back face deformation, velocity and acceleration of back face deformation, and in-plane strain measurements. Previously at the U.S. Army Research Laboratory (ARL), DIC has been used by Yu et al.(*6, 7*) and Weerasooriya (*8*) to measure transient deformation of the back surface of composite material and experimental helmets during impact. Their purpose was to collect transient displacement and strain history data to improve understanding of various materials and advance their finite element analysis (FEA) models.

By using DIC to collect helmet BFD data, it is possible to compute a new helmet performance metric; the "available energy" that might be potentially imparted to a Soldier's head. Thus, a new experimentation methodology to test and evaluate helmet BFD characteristics that is dynamic and previously correlated to injury will be presented. This approach advances the state-of-the-art in helmet BFD evaluations from using only static, post-impact metrics (deformation into clay) to dynamic, fully profiled (volume, velocity, etc.) helmet BFDs.

2. Objectives

Ballistic impact to a Soldier's helmet by small arms is typically seen as a high-speed, low-mass impact. However, when a composite helmet is used as protective equipment, the ballistic impact transferred to the Soldier's head is lessened to a lower speed, slightly higher mass impact caused by helmet BFD.

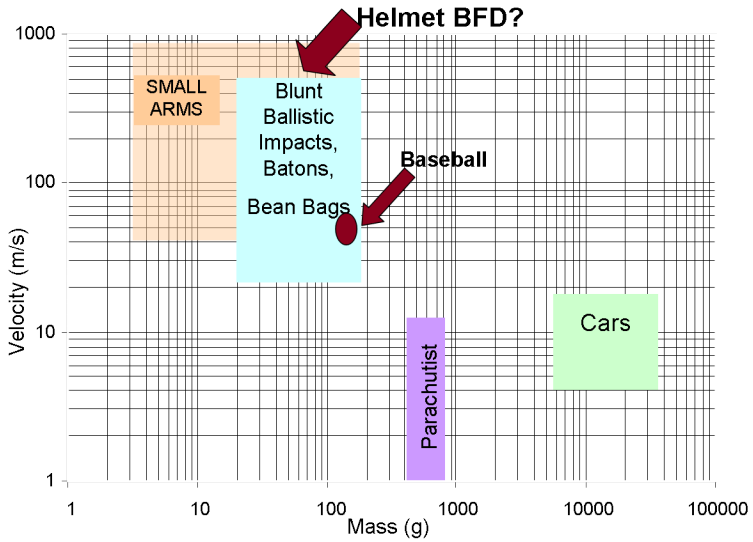

Figure 2: Hypothesis question: Is helmet BFD similar to blunt impact?

As shown in figure 2 (*9*), we want to test the hypothesis that helmet BFD mechanically loads the skull similar to a direct impact from a less-than-lethal projectile or blunt object impact.The benefit of relating helmet BFD to blunt object impact is to take advantage of the more prevalent data that exists for relating the tolerance of the head to blunt, non-lethal impacts as developed by the automotive, sports, and law enforcement communities.

The objectives of this program are to: 1) gain experience with, and demonstrate the utility of DIC as a tool to enable calculations of the energy required for the blunt criterion injury metric and 2) test the hypothesis that helmet BFD mechanically loads the skull similar to a direct impact from a less-than-lethal projectile or blunt object impact.

3. Approach/Methods

ARL has a well-established history of experimentation expertise to measure and characterize small arms ballistic impacts on many types of armor. In current helmet experimentation, it is routine to test for perforation/no perforation, V_0, and V_{50} ballistic resistance metrics. These metrics are determined from a series of ballistic shots, executed for a specific threat and helmet using methodology described in NIJ-STD-0106.01 (*10*), MIL-STD-662F (*11*) and the modified Langlie Users Manual (*12*). Complete or partial penetration data are only required to calculate these static metrics. In this study, a new test methodology for obtaining dynamic (vice static) impact metrics for ballistic helmet BFD is examined.

3.1 Criteria to Predict Blunt Impact Injury and Guide Experimentation

Some experimental measures have been developed by the automotive and sports industries to assess injury risks for low speed, high mass impacts. Criteria such as head injury criteria (HIC), viscous criterion, angular rotation thresholds, translational acceleration limits, and head impact power have been proposed. It is commonly accepted that skull fracture can be related to maximum dynamic force; however, there is no consensus on the criteria to use to cover the full spectrum of possible head injuries.

Sturdivan (*13*) states that no one injury model works well across the spectrum of blunt head and neck injuries due to the different mechanisms that are potentially involved. Sturdivan describes the four basic injury mechanisms as the following:

- Skull fracture, with damage to the underlying tissue (brain, cranial nerves, blood vessels).
- Shear injury from rapid rotation of the skull combined with a lagging rotation of contents.
- Cavitation caused by differential acceleration of the skull and its contents.
- Fractures to the cervical spine, connective tissue injury, and spinal cord injury from bending or twisting stress caused by the differential motion between the head and trunk.

Sturdivan indicates the physical quantity that properly expresses the capacity to do work on tissue and cause damage from blunt impact is energy. He proposes the blunt criterion (BC) as a prospective measure to predict head injury from blunt, less-than-lethal projectiles.

$$BC = ln\left(\frac{E}{T * D}\right), \tag{1}$$

where E is the impact kinetic energy in Joules, D is the diameter of the projectile in centimeters (if impact area is circular), and T is the thickness of the skull in millimeters.

The BC has been demonstrated to correlate very well with experimental data published from cadaver and animal studies *(5–7)*. Until more input from the medical community and independent validation of injury models are performed, we believe the BC will provide a good starting point for injury correlations due to helmet BFD. Therefore, we strive to develop next generation ballistic helmet test methodology for non-penetrating impacts that allows us to measure the energy required for BC calculations in addition to maximum dynamic force.

3.2 DIC Concepts

DIC is a promising technique that can measure area or volume of back face deformation, rate of back face deformation (velocity), and acceleration. The DIC system used in this study was developed by GOM Optical Measuring Techniques of Braunschweig, Germany and utilizes a software package called ARAMIS (*16*).

Three-dimensional DIC uses two high-speed cameras to stereoscopically track the movement of a grey scale or dot pattern in space. For this study, a dot pattern is applied to the inside surface of a helmet with padding and harnesses removed. During ballistic impact of the helmet, the cameras and software track changes in the dot pattern. The 3-D coordinates of specific surface locations are determined, and the movement of those discrete locations relative to each other over time is computed. In the DIC software, any single data point within the dot pattern can be selected and its time history displayed. The time dependent values of the entire surface of data points can be exported and post-processed as needed. This is a powerful technique for capturing dynamic deformation, volume, velocity, and acceleration data. DIC is well-suited for 3-D displacement measurements under static and dynamic load in order to analyze deformations and strain.

3.2.1 Calibration

To measure helmet BFD, the deforming helmet surface needs to stay within a calibrated measuring volume. The calibrated measuring volume is mapped out by moving National Institute of Standards and Technology (NIST)-traceable calibration panels with refererence points through space in a predetermined sequence. As part of the calibration process, the distance between the cameras and the orientation of the cameras relative to each other is determined. Using the two-dimensional (2-D) camera images, the software triangulates the 3-D coordinates of the reference points. The calculated 3-D coordinates are “calculated back” again into the 2-D camera coordinate system. The difference between the original and recomputed 2-D camera coordinates is called the reference point deviation. The calibration deviation is calculated from the average reference point deviation of all points recorded during the calibration process. For correct

calibration, calibration deviation should be between .02 and .08 pixels (*16*). Decalibration may occur if any changes are made to the cameras' positions or focal lengths.

3.2.2 Noise Floor

A noise floor measurement, shown in figure 3, should be made preliminary to any testing. This noise floor determination will show the level of ambient environment (temperature, vibration, air currents) and testing system noise. The noise floor measurement is made using the identical setup of the test situation; i.e., target is mounted as in the actual test, lighting and camera settings are made identical to actual testing environment, target surface preparation is made as in the actual test. The video acquisition is done as though measuring an actual event by collecting about a dozen or more frames of video for the noise floor measurement.

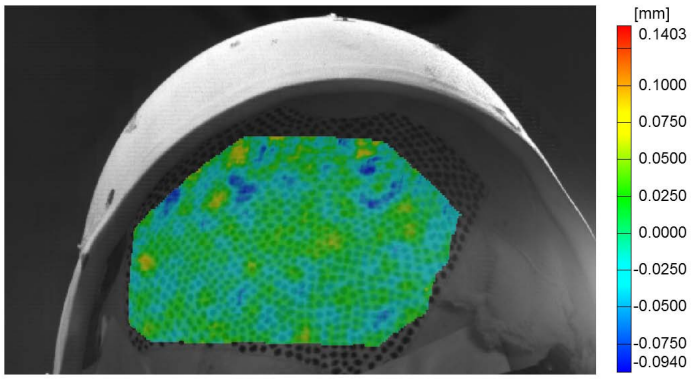

Figure 3. Noise floor measurement.

In practice, a noise floor can be collected during any test, as the stages prior to any target deformation, by saving a few frames of the video before impact. At this point in the DIC system setup, we are interested in observing and diagnosing any unusually high level of noise with an attempt toward attenuating its source.

In figure 3, the highest level of noise deformation at any point on the surface, relative to the zero stage, is shown as the maximum value at either end of the auto-scaled index. This value should be relatively low, compared to the expected deformation of the target upon testing. In this sample stage, the maximum noise deformation is 0.140 mm which is about 0.6 % of the expected deformation of 25 mm. How low the noise floor level should be depends on specific test requirements and engineering judgment.

3.3 Gaining Experience with DIC using Pendulum Impacts

In order to gain experience with DIC, pendulum impacts on cardboard and copper plates were performed. The impacts produced a dynamic bulge formation in the plates that was tracked using

DIC and then compared to FARO®* arm measurements. From these experiments, familiarity with the software, cameras, lighting and deforming surface preparation were obtained.

3.3.1 Pendulum Impacts on Cardboard

As a preliminary step in our analysis of the DIC system, steps were taken to record and measure the deformation created by dropping a pendulum onto a piece of conventional corrugated cardboard. The virtue of a pendulum is that it can provide consistent impact energies from a given release height; therefore, comparisons can be made between impacts onto various targets.

A one-foot-square piece of corrugated cardboard was attached to a sturdy steel frame by clamps at the four corners. A hex bolt was attached to the face of the pendulum bob and the head of the bolt was aligned to impact the center of the cardboard squarely. The noise floor measurement previously mentioned was done and found acceptable.

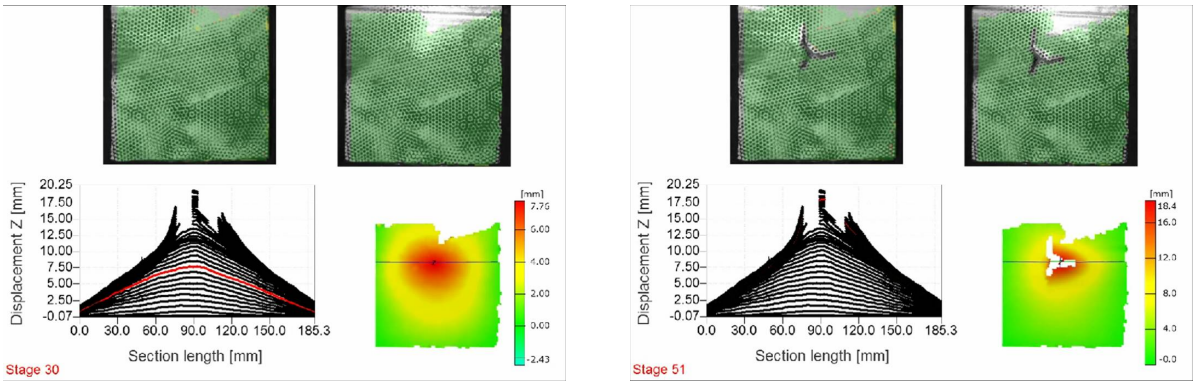

(a) (b)

Figure 4. DIC image for cardboard impact (a) before tearing (b) after tearing.

Figure 5 shows DIC images for the cardboard impact before and after tearing. The upper images show the left and right camera views, respectively. The bottom right images show surface deformation contour plots. The black line across the middle of the surface contour plots highlights where data is collected to produce the displacement versus section length data shown in the bottom left images. The displacement versus section length contours start at zero time and increase in time until the contours show rupture.

The bulge formation in the cardbord was tracked up to the point where the cardboard ruptured. Even after the cardboard developed a tear, the DIC software did an excellent job of computing the data around and up to the rupture. Comparison of the tear computed by the DIC software and the tear captured by the camera images reveals a very similar pattern.

3.3.2 Pendulum Impacts on Copper

Next, pendulum impacts were done on a 1-ft^2 sheet of 0.0625 in copper plate. It was also mounted to the stand by the four corners with clamps, and was impacted by the bolt head of the

*FARO is a registered trademark of FARO Technologies, Inc.

pendulum bob. Using a copper sheet allowed us to measure and compare the static deformation after impact between the DIC system and the FARO® laser measuring system. The FARO® arm provides the capability to make surface measurements and dimensional calculations with a high degree of accuracy. Thus, it provides an excellent verification of DIC measurements for static deformations. We assume, after a large number of time steps after impact, the test surface comes to rest at its final static deformation.

Figure 5 shows the post-drop surface image, z-axis deviation and difference between the DIC and FARO® surface deformation results. DIC and the FARO® arm produced maximum deformation results of 6.19 and 5.74 mm, respectively. The average deviation between the two techniques was found to be +0.063 -0.171 mm.

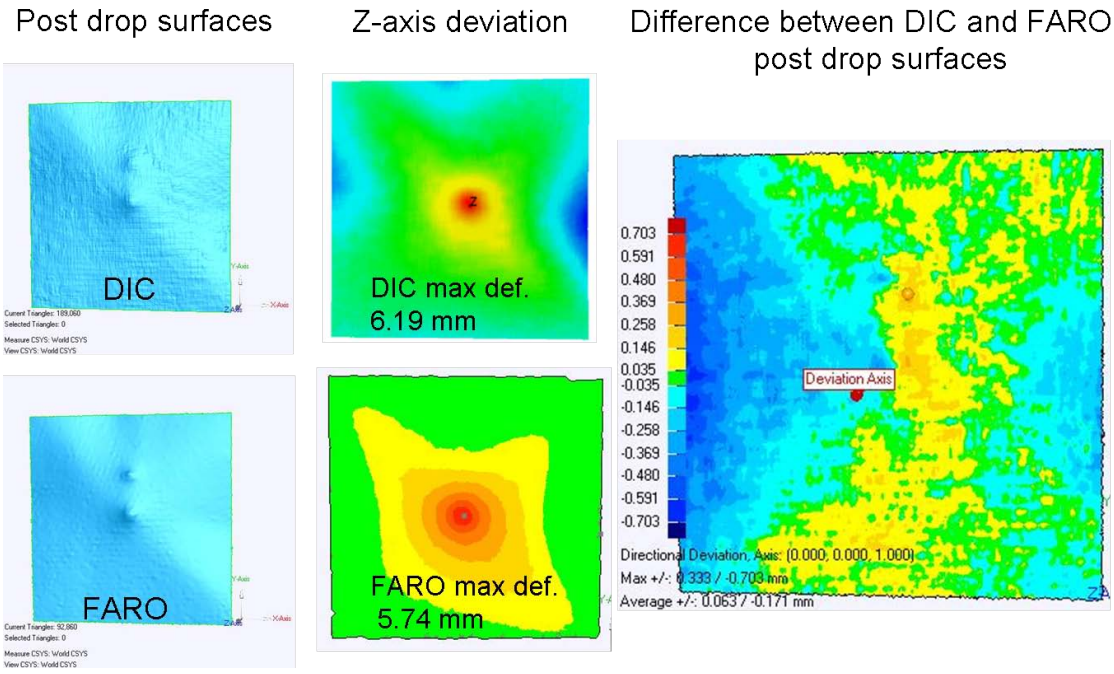

Figure 5. DIC and FARO® images for copper plate impact.

3.4 Range and DIC Set-up for 9 mm Impacts on Helmets

After the pendulum impacts, DIC experiments were conducted with 9 mm rounds impacting helmets. For non-perforating 9 mm shots against a helmet, the range schematic is as shown in figure 6. Two high-speed video cameras are positioned above the test area. From a top view, the cameras are positioned 15° apart. Their lenses are focused on the expected area of impact.

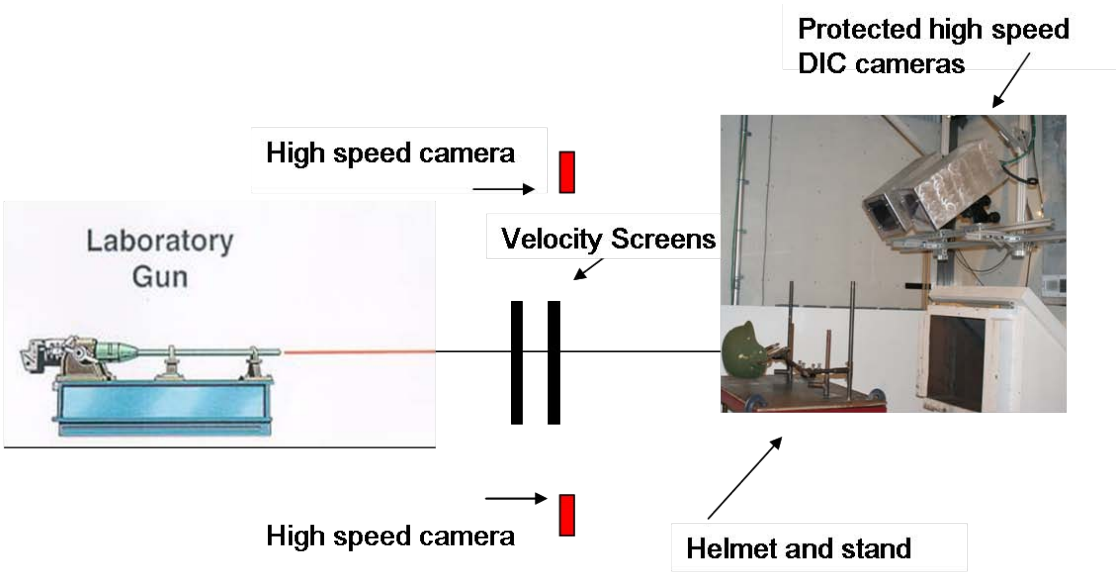

Figure 6. Range schematic for 9mm shots against helmets.

Additional details pertinent to the firing sequence are as follows:

- Gun was a 9 mm Aero tube, 8.25 in long, 1:10 twist, 6 groove (Bill Wiseman .357 Mag number: 1), fired by solenoid.
- Muzzle to target distance of 254.5 in.
- Triggering screens were 4 in diameter (Whithner #0303375D00) held in a custom built holder with 0.500 m separation. Average velocity at the midpoint between screens determined by dividing the 0.500 m separation by the time interval.
- Second screen to target distance of 50.5 in.
- Time intervals were measured using Agilent universal counter model 53131A (225 MHz, s/n: MY47003526). The time intervals are sent to a LabVIEW program to display velocity in ft/s and m/s. The program also records range temperature and humidity as well as: shots per barrel, projectile, propellant type, and load.

3.4.1 Helmet Mounting Technique

A single clamp to secure the helmet was initially tried, but did not work because often the impact would cause the helmet to move with the deformation. A more secure clamping of the helmet was used to reduce the effects of impact momentum. The ARAMIS software has the capability to compensate for full body motion such that only local deformations are tracked; however, for simplicity and repeatability, we secured the helmet to prevent full body motion. In the future, boundary conditions that better emulate the biofidelic neck movement of a Soldier are desirable.

3.4.2 Surface Preparation, Dot Pattern, and Lighting

In order to prepare helmets for DIC testing, the interior surface of the helmets were lightly sanded to remove any loose paint present that might fly off during ballistic impact. Then, an ink dot pattern was applied to the helmet's interior surface where deformation was expected to occur. Initially, the dot pattern was applied by hand using permanent ink markers. This process worked well, but was found to be labor intensive and tedious. Subsequently, an ink tattoo was developed by the ARAMIS technical representative for our use. The ink tattoo was found to work as well as the hand-applied ink dots, but with significantly less application labor. One difficulty encountered when attempting to use DIC on a helmet is getting optimal lighting to illuminate the curvature of the helmet interior where deformation is expected to occur. The high-speed camera images taken during DIC data collection required camera speeds of 50,000 frames per second and shutter speeds of 1/(frame speed) seconds. At these camera speeds, an intense light source is needed to uniformly illuminate the helmet surface without introducing glare or shadows. Light source placement was achieved through trial and error while taking noise floor images.

4. Results and Discussion

4.1 Overview of DIC Tests for 9 mm Shots Against Helmets

A total of fifteen 9 mm shots against large and extra-large size helmets (noted in comments in table 1) were performed to the left, right, front, back, and crown locations of the helmets as described in NIJ-STD-0106.01 (*10*). The bullet velocities were in the range of 1215$\pm$ 25 ft/s, which is slightly above the required velocity range of 1175 $\pm$ 50 ft/s indicated in the NIJ standard. The total yaw was less than 5° for all cases. The impact kinetic energy of the rounds were in the range of 555 $\pm$ 25 J. Details of the impact conditions are provided in table 1.

Table 1. Summary of helmet tests.

ID	Location	Impact Velocity (ft/s)	Impact KE (J)	Comments
1	Back	1234	569	X-Large
2	Back	1222	563	Large, Delaminated
3	Back	1239	579	Large
4	Back	1223	564	X-large
5	Back	1211	553	X-large
7	Crown	1218	558	Large
8	Crown	1208	548	X-large
9	Crown	1205	544	Large
10	Crown	1227	564	Large
12	Left	1209	547	Large
13	Front	1216	554	Large
15	Front	1207	545	X-large
16	Right	1213	550	X-large
17	Left	1195	534	X-large, Delaminated
18	Right	1207	545	Large, Delaminated

Data could not be collected (dots required for DIC flew off or disappeared) for shots 6, 11, and 14 (missing in the table) due to surface preparation or delamination issues. In some cases, the comments in the table indicate the final layer of composite material delaminated during the BFD of the helmet. Delamination is the separation between fibers and the matrix material of a composite material. Delamination of the final layer of composite material typically occurs when BFD is centered on a seam present in the final layer of the helmet.

4.2 Available Energy for Potential Impact to Solider's Head

The process of small arms penetration into compliant, composite laminates as described by Cheeseman and Bogetti (*17*) is shown in figure 7. The bulging of the back surface illustrates the helmet BFD we are replicating and measuring. For non-perforating impacts, the remaining plies of composite material eventually stop the bullet, but not always before the bulging area of the helmet impacts the Soldier's head with significant force. The bulging area impacts the Soldier's head from the helmet standoff distance until the point of maximum helmet BFD. During this process, it would be useful to know the available energy that could be potentially deposited into a Soldier's head as a predictor of injury.

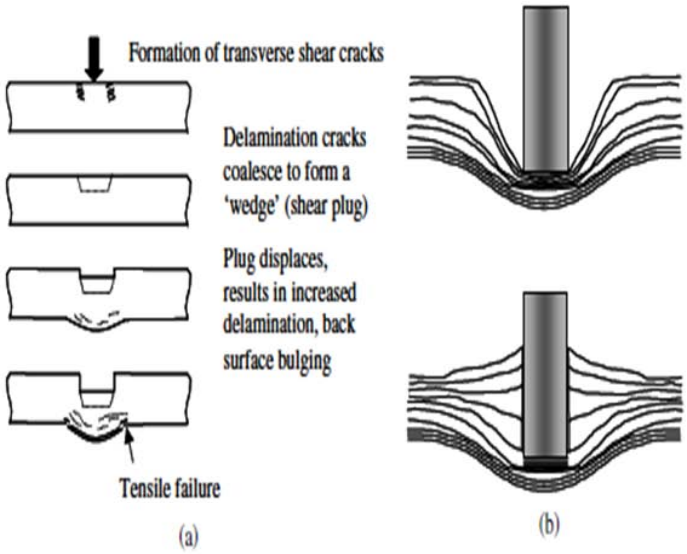

Figure 7. Process of small arms penetration into a composite laminate.

In figure 8, the interior composite plies of a shot helmet can be seen. The helmet was dissected to reveal the delamination of the interior composite layers. We were able to extract the mushroomed 9 mm bullet that was captured in the composite layers. The back surface of the bullet is shown in the left of the image. Also, the side view of the dissected helmet reveals the bulging of the back surface and cavity that results after coming to a static resting point. The cavity at the top of the figure is from a different shot.

Figure 8. Dissected helmet and mushroomed 9mm bullet.

4.3 Using DIC Measurements to Calculate Energy for Blunt Criterion

As indicated by equation (1), the blunt criterion is a function of impact kinetic energy, thickness of the skull, and projectile or blunt object effective diameter (the diameter of the contact area between the skull and the striking surface). The average thickness of the skull used in this study is 6.8 mm. By using DIC to collect helmet BFD and velocity data, it is possible to compute the available energy that might be potentially imparted to a Soldier's head. The available impact energy in a differential area of helmet surface is equivalent to the kinetic energy that the helmet area possesses when it deforms to the helmet standoff distance (0.5 in). This available energy quantity can be used to calculate the blunt criterion metric, which in turn provides a prediction for AIS levels and skull fracture.

$$E = \text{Available Energy}_{\text{BFD}} = E_{\frac{1}{2}\text{in}} - E_{\text{max def}} \tag{2}$$

$$E = \int F(x)\,dx = \int F(t)\,v(t)\,dt \tag{3}$$

$$E = \int m(t)\,a(t)\,v(t)\,dt \tag{4}$$

$$E = \int_{\text{max def}}^{\frac{1}{2}\text{in}} \rho(t)\,Vol(t)\,a(t)\,v(t)\,dt \tag{5}$$

$$E = \frac{1}{2}\rho\,(t)\,\text{effective area}\,(t)\,\text{v}^2\,(t)\,|_{\text{max def}}^{\frac{1}{2}\text{in}} \tag{6}$$

As shown in equation (5), the available energy from helmet BFD can be computed where ρ is the areal density of the remaining plies of helmet after partial penetration of the round. For this study, ρ is set to 1.5 lbsf, three-fourths its typical value of 2.0 lbsf, to approximate the plies remaining after ballistic impact. In future work, better estimates of the remaining plies after impact will be obtained by x-ray or helmet dissection. In equation (5), Vol is the volume, a is the acceleration and v is the velocity of the helmet BFD region.

However, it is computationally simpler to use the instantaneous velocity as provided by DIC measurements rather than integrate to find it. It is also more accurate, since acceleration values are a) subject to far more error, and b) instantaneous velocity is more representative of what was actually measured, i.e., displacement. Thus, we obtain the instantaneous energy by computing $\frac{1}{2}$ $m(t)$ $v^2(t)$ where $m(t)$ is computed from ρ times the area associated with the effective diameter as shown in equation (6). The mass of the bullet is also included in $m(t)$. Thus, the available energy is accumulated from $\frac{1}{2}$ in., reached at 220 μsec in figure 9a, to maximum deformation at 740 μsec in figure 9b for a sample case (shot 16 in table 2).

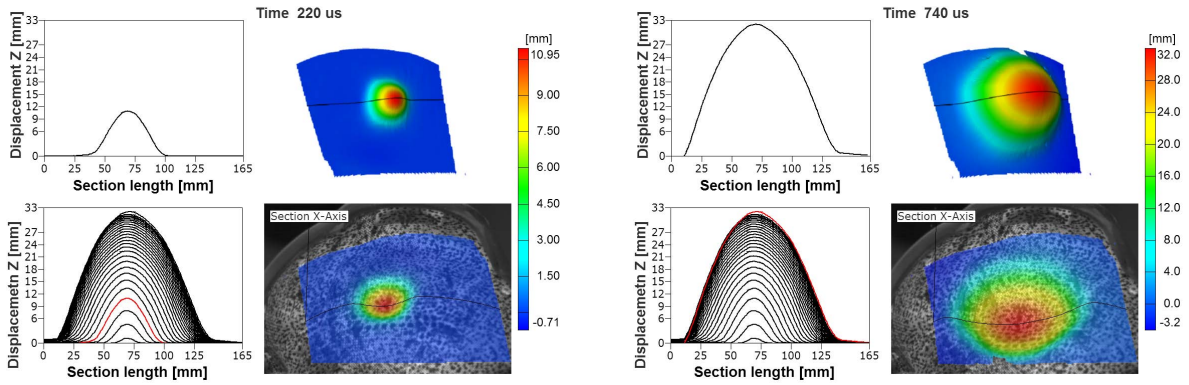

(a) (b)

Figure 9. DIC deformation contours for 9 mm impact (a) at helmet standoff (b) at maximum deformation.

In figure 10a, the three red x's show the values of displacement, velocity, and acceleration, respectively, for a point located at the center of the bulge area (reference point 1), at 220 μsec. The red x's in figure 10b show the values of the same variables at 740 μsec. With the postprocessing available in ARAMIS, the data for all points within the deforming surface bulge can be output to a text file. Then, the data for displacement, velocity and acceleration can be graphed with respect to time or postprocessed using a MATLAB program to produce the available energy from helmet BFD.

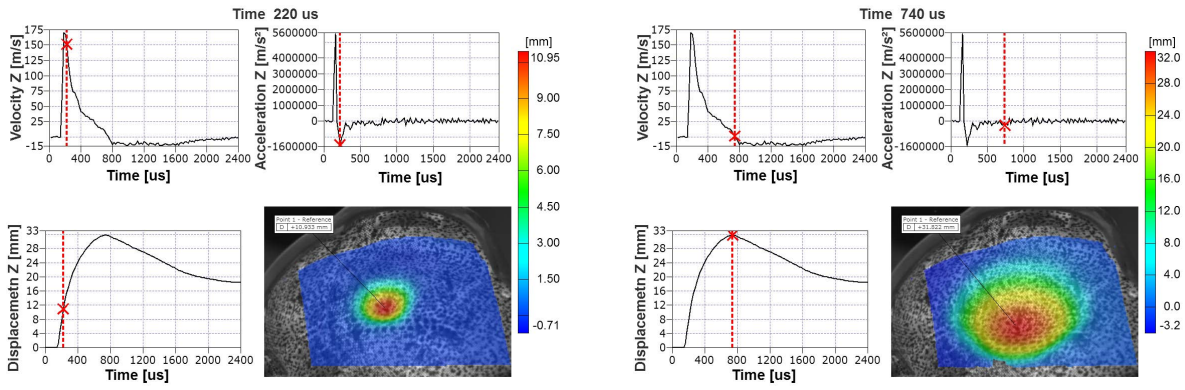

(a) (b)

Figure 10. DIC time histories and surface contours for 9 mm impact (a) at helmet standoff (b) at maximum deformation.

4.4 BFD Velocity Surface Plot

Shown in figure 11 is a surface plot of maximum velocity for shot 16 of 2,939 surface points after each point crossed the 0.5 in standoff distance. These velocities were typically decreasing as they passed the standoff distance, which is consistent with the process of the composite fibers retarding the forward motion of the projectile until a point of maximum deformation is reached. After the point of maximum deformation, the deforming surface often rebounds as seen in high speed video and the last frame of figure 1. The velocity is an important parameter as it is the dominant factor in calculations for the available energy used to compute the BC.

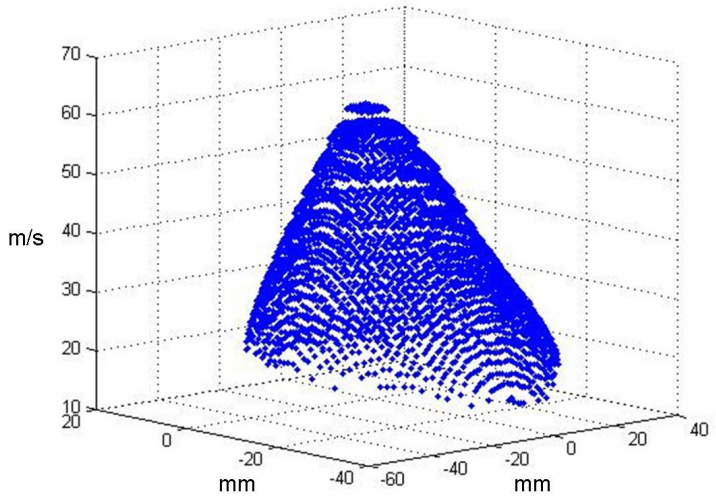

Figure 11. BFD velocity surface plot.

4.5 Summary of Helmet Results

In table 2, DIC results are summarized and the BC is calculated for the 9mm versus helmet shots conducted in this study. At the time of maximum BFD, we can determine from DIC data the projected area of impact to a Soldier's head. We then compute an equivalent circular area from which the effective diameter is determined. The maximum velocity typically occurs after impact and well before the point of maximum BFD as seen in figure 10b. Maximum z-axis deformation is the distance from a point on the surface of the helmet to its location at maximum deformation along the direction of deformation. The available energy, effective diameter, and BC are computed assuming a helmet standoff distance (gap) of 0.5 in and 0.75 in. The actual standoff distance of a helmet to a Solider's head depends on pad thickness and personal anatomy and in reality is probably somewhere between these two distances. Therefore, the actual available energy and BC values also probably fall between the values noted in the chart for helmet standoff distances of 0.5 in and 0.75 in.

Also evident from the table is that crown shots result in lower BC values than shots to the front, back or sides of the helmet. The crown of the helmet is stronger than the other sides due to its inherently flatter geometry. Also, the composite layers in all areas except the crown have been cut to accomodate the manufacturing process required to mold flat sheets into the final curved helmet geometry.

Very little can be said about the spread of the data shown in table 2 for similar helmet locations. The helmets used in this study were not from the same lot number or even necessarily the same manufacturer. They were excess helmets previously turned in to the Defense Reutilization and Marketing Services (DRMS) and used by this project to simply study feasibility of the methodology and techniques tested herein. In future efforts, it would be desirable to obtain unused helmets from the same manufacturer with the same lot number for all tests.

Table 2. Summary of helmet results.

ID	Max Velocity (m/s)	Available E (J)		Max Z-Axis Def (mm)	Eff Diameter (cm)		Max BC (X)	
		.5"gap	.75" gap		.5"gap	.75" gap	.5" gap	.75" gap
1	189.20	243.17	132.19	35.86	5.33	4.40	2.00	1.51
2	188.28	268.47	89.30	33.97	4.92	3.91	2.20	1.57
3	169.32	206.04	85.30	38.97	5.41	4.78	1.86	1.07
4	184.61	264.55	126.47	39.48	5.51	4.74	2.04	1.45
5	177.14	203.43	55.50	29.83	4.74	3.67	2.00	0.97
7	165.74	94.33	16.99	24.27	4.33	3.07	1.58	-0.13
8	172.09	128.03	42.63	28.42	4.66	3.65	1.51	0.65
9	154.97	121.81	23.71	25.99	4.64	3.58	1.48	0.09
10	160.69	105.47	25.95	25.35	4.54	3.25	1.34	0.25
12	157.42	158.94	43.63	29.32	4.78	3.76	1.74	0.63
13	217.42	340.29	134.04	42.81	5.83	4.60	2.37	1.70
15	180.22	207.68	95.36	39.07	5.33	4.65	1.95	1.27
16	170.62	195.22	61.24	32.07	4.94	4.05	1.95	1.01
17	183.90	228.11	95.53	35.60	5.45	4.55	2.02	1.30
18	167.66	220.79	93.37	38.78	5.12	4.28	1.96	1.27

In Sturdivan (*13*), the mean is the value of the model variable for which the predicted probability

of occurrence is 50 %. He describes the skull mean as equivalent to the energy-based BC. Sturdivan computes BC values using data from 25 to 28 gram impactors versus rehydrated skulls, filled and coated with 20% gelatin. For AIS levels of 2, 3, and 4, BC values reported by Sturdivan were 0.5667, 0.8081 and 1.0527, respectively. Fitted mean BC values ranged from 0.323 for AIS level 1 to 1.538 for AIS level 6. From table 2, Our BC values primarily fall in the same range as Sturdivan's reported values, although some values are higher, particularly for the 0.5 in helmet standoff distance. Raymond et al. (*15*) report a 50 % risk of skull fracture for BC values greater than 1.61. However, Raymond used a slightly modified version (added $M^{\frac{1}{3}}$ multiplier to denominator where M is mass of struck cadaver) of Sturdivan's BC. Raymond's average BC value was 2.12, obtained from fourteen direct impact tests of blunt objects against cadaver skulls. In this study, we are approximating helmet BFD as an equivalent blunt object, and find it promising that our BC values fall in the same range as their experiments.

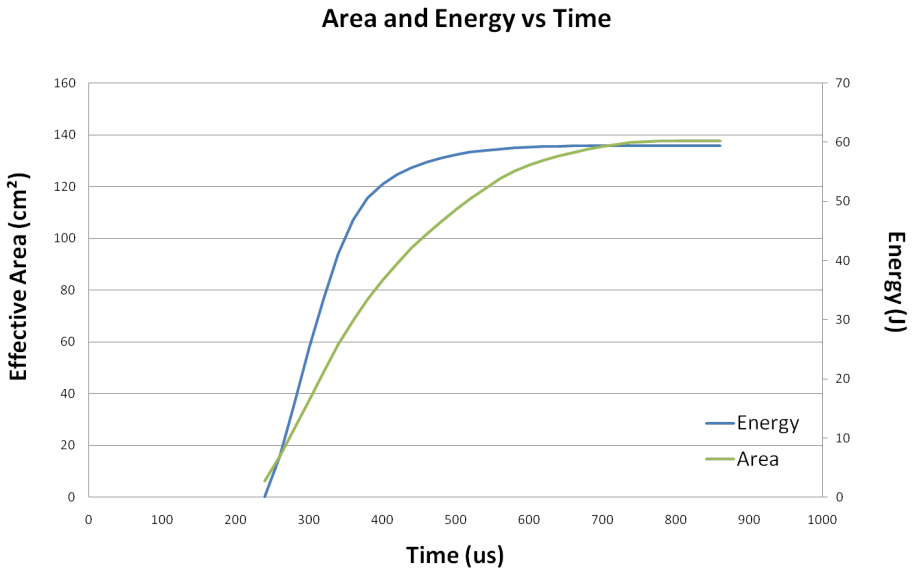

Figure 12. Cumulative available energy, effective area and BC time histories.

In figure 12, cumulative available energy and effective area as a function of time are provided for shot 16. The average BC between the .5 and .75 in data was computed to be 1.48. The trends in these time histories are representative of the other shots as well. We note the effective area continues to increase with time although the available energy levels off at an earlier time. As previously mentioned, from DIC deformation and velocity versus time charts (see figure 10b), the velocity peaks and actually starts to decrease well before the maximum displacement is reached, thus supporting the trend found here in the available energy. Velocity is the predominant variable influencing the available energy and BC results. Although the area continues to increase, the energy has leveled off meaning very little additional injury probably occurs at latter times and at the point of maximum deformation. The more important time period is right after the initial impact of helmet BFD when velocity and its contribution to available energy is the highest.

4.6 Similarity of Helmet BFD to Blunt Object Impact

When the helmet BFD data collected as part of this study is plotted on the log-log plot of velocity versus mass, it falls in the same realm of data as that of blunt object impact (see figure 13).

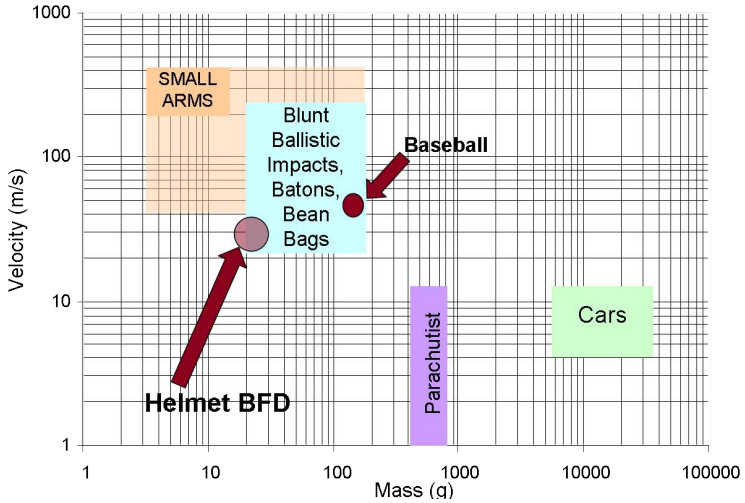

Figure 13. Helmet BFD similar to blunt object impact.

For the 9 mm threats and helmets tested in this study, the data confirms our original hypothesis that helmet BFD mechanically loads the skull similar to a direct impact from a less-than-lethal projectile or blunt object impact.

5. Conclusions

An experimentation technique that replicates the helmet and Soldier's head as a system and can accurately replicate biofidelic loading and response is desirable. However, our current understanding of composite materials, varying properties of the human skull from person-to-person, and the many ways helmet manufacturers can use composites under performance-based standards makes the problem intractable. Also, experimental methodology is desirable that predicts injury potential using biofidelic, durable, repeatable and calibrated techniques. However, experimental methodology that is both biofidelic and durable when impacting a fragile human skull or its surrogate is problematic.

Digital image correlation is a desirable experimentation technique that can be used to accurately capture BFD area and rate of deformation for a helmet undergoing impact from a small arms round. As the helmet deforms from the standoff distance to its point of maximum BFD deformation, these data can be used to calculate an available energy that could potentially impact a Soldier's head. Thus, DIC is an excellent helmet experimentation technique for providing accurate helmet performance data that will allow increased understanding of BFD and quanitative

assessment and validation of helmet performance results. The added complication of determining how this available energy is actually absorbed by the Soldier's head, is not necessary to provide a first order, conservative estimate of injury potential. It may be desirable to bring down this conservative estimate by developing correction factors for pads, and other energy absorption liners.

For the 9 mm threats and helmets tested in this study, the DIC data confirms our original hypothesis that helmet BFD mechanically loads the skull similar to a direct impact from a less-than-lethal projectile or blunt object impact. Thus, if we assume all the available energy from helmet BFD is absorbed by the head, the resulting blunt criterion calculation provides a conservative prediction of AIS levels and skull fracture.

Finally, a new experimentation methodology to test and evaluate helmet BFD characteristics that is dynamic and correlated to injury has been presented. Utilizing DIC data, a new metric, available energy for potential impact to a Soldier's head, has been developed that allows one to compute a conservative estimate of the blunt criterion. This experimentation methodology advances the state-of-the-art in helmet BFD evaluations from using only static, post-impact metrics (deformation into clay) to dynamic, fully profiled (volume, velocity, etc.) helmet BFDs.

6. Recommendations

In this study, estimates of the areal density of the remaining plies of composite material after non-perforating impact were made in order to compute the BC. In the future, the areal density will be more accurately determined using x-ray or helmet dissection. Another methodology improvement would be to mount the helmet with boundary conditions that simulate how the helmet is actually constrained when worn by a Soldier. Future studies should use helmets that are from the same manufacturer and have the same lot number. In future studies, it might also be possible to reduce the available energy that could potentially impact a Soldier's head by correction factors for pads, or other energy absorption liners.

The BC data produced by the methodology outlined in this report is compared to BC injury correlations previously performed by others. However, it would be more desirable to obtain injury correlations where our dynamic BFD data is used as the loading condition for post-mortem human subject tests.

The complex response of composite materials can potentially make the experimental characterization of helmet deformation expensive and time consuming. Therefore, a physics-based finite element analysis simulation capability will be pursued to supplement and validate our experimental data.

In addition, blunt trauma may also be caused by rapid translational and rotational accelerations/decelerations of the head with respect to spinal joints as a result of ballistic helmet impacts. Future work will focus on techniques for experimentally capturing these accelerations and making correlations to possible injury.

Finally, knowledge of the conditions leading to head trauma obtained through experimentation or numerical modeling should enable the selection of new energy-absorbing materials for helmets. The ultimate goal of future instrumentation and methodology efforts should allow helmet design candidate performances to be objectively evaluated. Test data and characterization of helmet response could then be used to achieve improved warfighter survivability.

7. References

1. Mahoney, P.; Ryan, J.; Brooks, A.; Schwab, C. *Ballistic Trauma, A Practical Guide*, second ed.; Springer-Verlag, 2005.

2. Cannon, L. Behind Armour Blunt Trauma - an emerging problem. *J R Army Med Corps* **2001**, *147* (1), 87–96.

3. Carroll, A.; Soderstrom, C. A New Nonpenetrating Ballistic Injury. 1st National Symposium on Traumatology, 1978.

4. H.P. White Laboratory Inc. Test Procedure for Bullet Resistant Helmet. *HPW-TP-0401.01B* **1995**.

5. http://www.briscoetechnologies.com/vest.

6. Yu, J.; Hsieh, A.; Dehmer, P.; Sands, J. *Real-Time Full-field Deformation Analysis on the Ballistic Impact of Polymeric Materials Using High-speed Photogrammetry*; ARL-RP-0290; U.S. Army Research Laboratory, 2010.

7. Yu, J.; Dehmer, P.; Yen, c. *High-speed Photogrammetric Analysis on the Ballistic Behavior of Kevlar Fabrics Impacted by Various Projectiles*; ARL-TR-5333; U.S. Army Research Laboratory, 2010.

8. Weerasooriya, T.; Moy, P. "Measurement of Full-Field Transient Deformation of the Back Surface of a Kevlar KM2 Fabric during Impact for Material Model Validation." *Proceedings of the 2008 International Congress and Exposition on Experimental Mechanics and Applied Mechanics*, Orlando,Florida, 2008.

9. Sherman, D.; Bir, C. An Overview of Human Effects of Less-lethal Kinetic Energy Rounds. Wayne State University Presentation to Personnel Vulnerability Workshop, Army Research Laboratory, APG, MD, 2009.

10. National Insitute of Justice. NIJ Standard for Ballistic Helmets. *NIJ Standard 0106.01* **1981**.

11. MIL-STD-662F. V50 Ballistic Test for Armor. Department of Defense Test Method Standard, 1997.

12. Collins, J.; Moss, L. LangMod Users Manual. ARL Internal Document, 2008.

13. Sturdivan, L. Injury Criteria for Blunt Impact to the Head. Draft Report, 2005.

14. Sturdivan, L.; Viano, D.; Champion, H. Analysis of Injury Criteria to Assess Chest and Abdominal Injury Risks in Blunt and Ballistic Impacts. *The Journal of Trauma Injury, Infection, and Critical Care* **2005**, *56*, 651–663.

15. Raymond, R.; Van Ee, C.; Crawford, G.; Bir, C. Tolerance of the Skull to Blunt Ballistic Temporo-parietal Impact. *Journal of Biomechanics* **2009**, *42*, 2479–2485.

16. ARAMIS v6.1 User Manual. Gom Optical Measuring Techniques,Braunschweig, Germany, 2009.

17. Cheeseman, B.; Bogetti, T. Ballistic impact into fabric and compliant composite laminates. *Composite Structures* **2003**, *61*, 161–173.

INTENTIONALLY LEFT BLANK.

List of Symbols, Abbreviations, and Acronyms

ACH	Advanced Combat Helmet
AIS	Abbreviated Injury Score
ARL	U.S. Army Research Laboratory
BC	blunt criterion
BABT	Behind Armor Blunt Trauma
BFD	back face deformation
DAQ	data acquisition
DIC	digital image correlation
FEA	finite element analysis
FMJ	Full Metal Jacket
HIC	head injury criteria
HPW	Henry Packard White
ISO	International Organization for Standardization
LRHV	Long Rifle High Velocity
NIJ	National Institute of Justice
NIST	National Institute of Standards and Technology
TBI	traumatic brain injury

INTENTIONALLY LEFT BLANK.

NO. OF COPIES ORGANIZATION

1 Admnstr
Defns Techl Info Ctr
ATTN DTIC OCP (Electronic Only)
8725 John J Kingman Rd Ste 0944
FT Belvoir VA 22060-6218

1 DARPA
ATTN IXO S Welby
3701 N Fairfax Dr
Arlington VA 22203-1714

1 Ofc of the Secy of Defns
ATTN ODDRE (R&AT) (1 CD)
The Pentagon
Washington DC 20301-3080

1 US Army Info Sys Engrg Cmnd
ATTN AMSEL IE TD A Rivera
FT Huachuca AZ 85613-5300

1 Commander
US Army RDECOM
ATTN AMSRD AMR W C McCorkle
5400 Fowler Rd
Redstone Arsenal AL 35898-5000

1 US Army Rsrch Lab
ATTN IMNE ALC HRR Mail & Records Mgmt
ATTN RDRL CIM L Techl Lib
ATTN RDRL CIM P Techl Pub
Adelphi MD 20783-1197

ABERDEEN PROVING GROUND

NO. OF COPIES ORGANIZATION

1 US Army Rsrch Lab
ATTN RDRL CIM G T Landfried
Bldg 4600
Aberdeen Proving Ground MD 21005-5066

11 DIR USARL
RDRL SLB D
D Hisley
J Gurganus
A Drysdale
J Lee
S Williams
R Kinsler
J Polesne
R Grote
RDRL SLB W
W Mermagen
P Gillich
C Kennedy
N Eberius
L Roach
E Hanlon
RDRL WMT D
R Kraft
RDRL WMM D
S Walsh
L Vargas-Gonzalez
RDRL WMM E
P Dehmer
RDRL WMM B
J Yu